Mechanical and Microscopic Tests to Examine the Plastic Strain Developed in a Cyclically Loaded Steel Brace

繰返し載荷を受けたブレースに生じた塑性ひずみを検証する材料試験と検鏡試験

TWEMERIMANA Xavier
Division of Architecture and Structural Design
Laboratory of Structural Engineering, Research Group of Structural and Urban Safety Design

Abstract

This study investigates localized plastic strain and strength developed in a cyclically loaded steel brace. The research is based on a previous brace test, where local buckling and fracture occurred at the brace center with cracks initiated at the corners. The central portion of the deformed brace, together with an undeformed reference specimen was extracted and subjected to mechanical and microstructural tests to examine the plastic local deformation and strength variation. The results showed the measured plastic local strain at the brace corner and yield strength distribution across the brace half section. Finite element captured brace response; however, it showed need for calibration to reproduce test results and deformation behavior.

Keywords: Steel Braces, Cyclic Loading, Local buckling, Fracture, Microstructural Tests, Finite Element Analysis.

1. Introduction

Steel braces are widely used in seismically prone regions. Although their global cyclic behavior has been extensively studied (e.g., Abe et al. [1]), the mechanisms of fracture initiation remain insufficiently understood because they strongly depend on the development of localized plastic strain. Recent studies on microstructural characterization (e.g. Rui et al. [2]) particularly those employing Electron Backscatter Diffraction and mechanical testing, enable quantitative evaluation of plastic deformation through crystallographic misorientation parameters such as Kernel Average Misorientation (KAM). This study integrates brace-level response with microstructural observations and mechanical tests to quantify localized plastic behavior and to predict fracture mechanisms of cyclically loaded steel braces.

2. Test Plan

An experimental program conducted by Abe et al. [1] was adopted to investigate the microstructural properties of a steel brace previously subjected to cyclic loading. As illustrated in Fig. 1, a brace specimen with a slenderness ratio of 27.1 and a width-to-thickness ratio of 7.1 was selected. Fig. 2 presents the force-displacement relationship of the brace specimen. The brace experienced local buckling at the mid-length and subsequent fracture at the corner of the cross-section at normalized displacement excursions of 2.5% and -1.5%, respectively.

Fig. 3(a) shows the brace specimen after completion of the cyclic loading test. Slices 1 and 2 located 5 mm

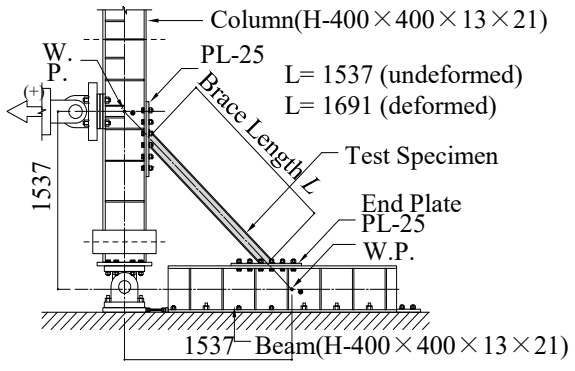

Fig. 1 Brace Test Setup (Source: Abe et al. [1])

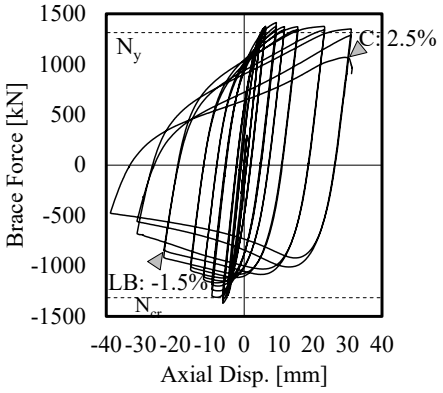

Fig. 2 Hysteresis of brace (Source: Abe et al. [1])

and 8 mm from the mid-length of the brace specimen, respectively, were extracted for microscopic examination. As illustrated in Fig. 3(b), Slices 1 and 2 were subdivided into Specimens A through P to investigate the plastic strain developed near the mid-length using microscopic and mechanical tests. Specimens A and P were subjected to electron backscatter diffraction (EBSD) test to measure the crystal misorientation in the circumferential and longitudinal directions.

In addition, Vickers' hardness tests were performed on Specimens B through M to evaluate material hardness. Four measurement layouts were adopted to investigate the influence of the number and spacing of indentation points. In Cases 1, 2, and 3, the minimum spacing between measurement points were 3.5 mm, 1.8 mm, and 1.8 mm, respectively. Case 4 was developed based on Case 3 by introducing additional indentation points with a minimum spacing of 0.8 mm in the localized region, in accordance with ASTM E92- 17.

To enable direct comparison between cyclically deformed material and its virgin condition, an undeformed steel section with identical material properties and geometric dimensions was subjected to the same testing procedure, as illustrated in Fig. 3(c).

3. Test results

Fig. 4 presents a contour map of the hardness distribution in Specimen L and provides a basis for determining an appropriate number and spacing of indentation points. In Case 1, which employed three indentation points through the thickness, variations in hardness were observed in the circumferential direction, whereas the hardness remained nearly constant through the thickness due to the limited number of measurement points. In Case 2, which used five indentation points, variations in hardness were partially captured in both the circumferential and thickness directions; however, the relatively large spacing in the circumferential direction limited the resolution of the distribution. In Case 3, with five indentation points distributed along the circumferential direction, clear variations in hardness were successfully identified in both directions. In Case 4, although localized increases in hardness were observed near the finely spaced indentation points, the overall hardness distribution was nearly identical to that obtained in Case 3. This indicates that the measurement procedure, particularly the spacing of indentation points, influences the

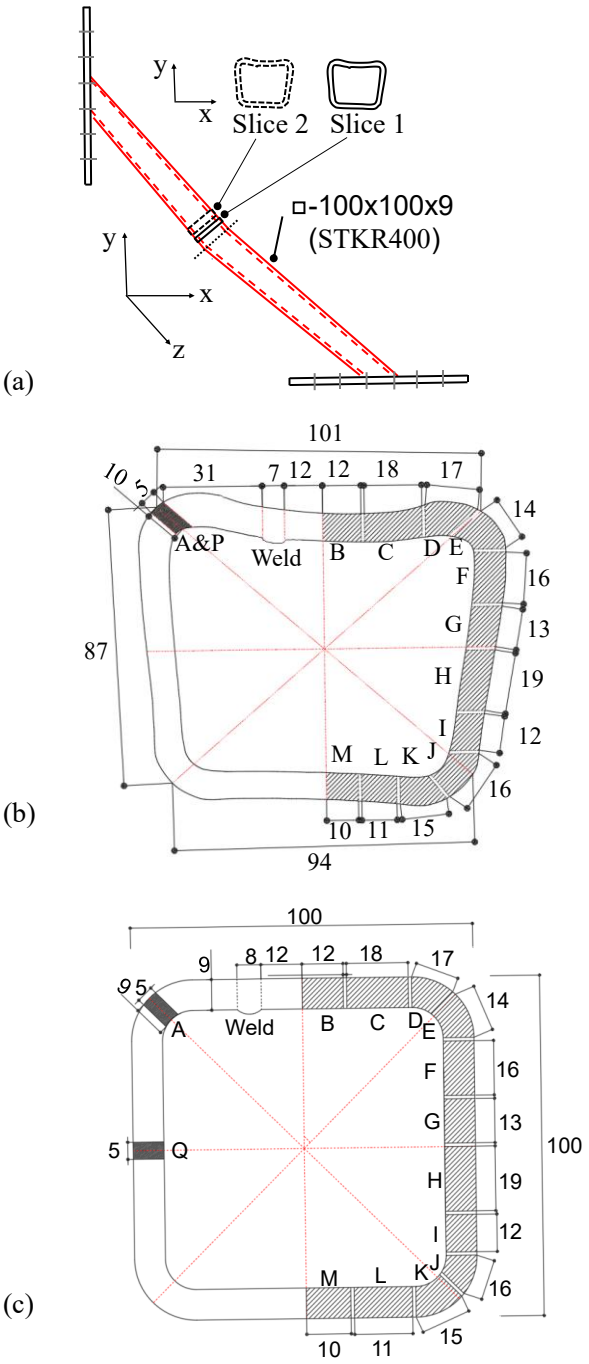

Fig. 3(a) Deformed Specimen after brace test, (c) Deformed slice 1 cutting plan for microstructural test; and (c) Undeformed slice 1 (dimensions: mm)

observed hardness distribution. Based on the observations, Case 3 was selected as an appropriate measurement scheme for evaluating the hardness distribution over the gross section of the brace.

Fig. 5 illustrates the hardness distributions of both the undeformed and deformed specimens is higher than that at the outer side of the section, which was attributed to the plastic rolling process used to fabricate

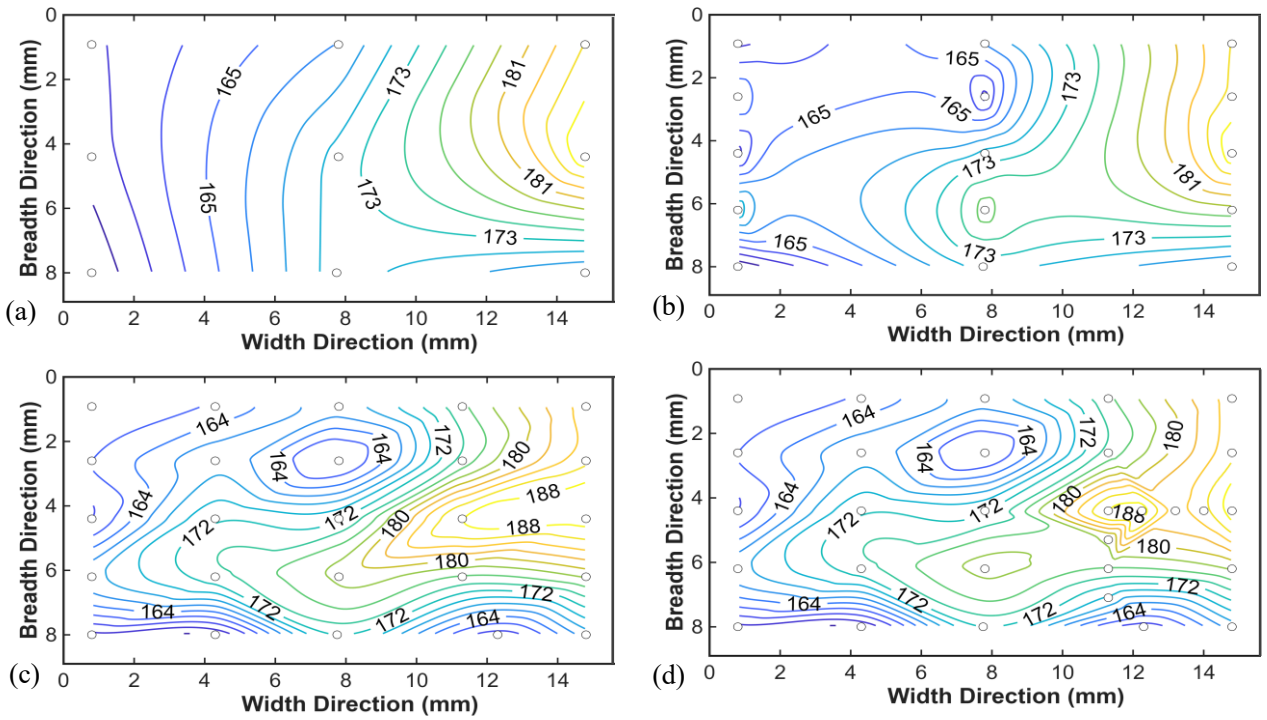

Fig. 4 Sampling Viability of Vickers Hardness Test, Specimen L: (a) Case 1, (b) Case 2, (c) Case 3; and (d) Case 4

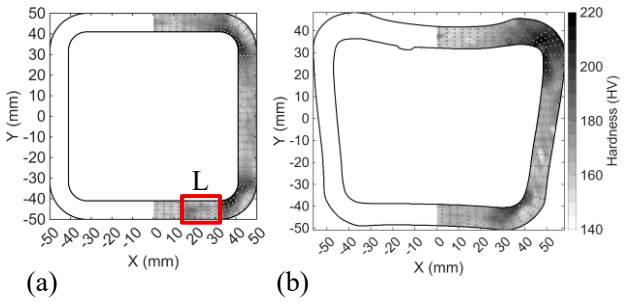

Fig. 5 Vickers Hardness results: (a) Undeformed Specimen; and (b) Deformed Specimen.

the square hollow section.

Fig. 5(a) presents the hardness distribution of the deformed specimen, where the hardness at the section corners was greater than in local regions. This corresponds to the cracking in deformed Slice 1 at the corner, where plastic deformation was locally concentrated.

Fig. 6 presents the microscopic test results for Specimen A, including kernel average misorientation (KAM), and the frequency distribution of KAM values obtained from EBSD analysis. The KAM maps represent the average local grain misorientations observed. KAM values in the undeformed specimen are close to zero in most regions, while those in the deformed specimen range from 2 to 5. Fig. 6(b) shows that the average KAM value increased from 0.610 to 1.30 after completion of the cyclic loading tests.

4. Discussions

In this study, plastic strains were evaluated using microstructural tests in conjunction with established correlations between crystallographic misorientation and local plastic strain. Based on the results of the Vickers hardness tests, the correlation proposed by Pavlina and Van [3] was adopted to estimate the yield strength from the hardness measurements. Kamaya [4] reported a linear relationship between local plastic strain and EBSD-based misorientation parameters, specifically the local misorientation M_L and step size d, as expressed in Eq. (1), subject to certain limitations.

$$\varepsilon_{p(local)} = \frac{M_L - 0.1}{-0.0027d^2 + 0.041d} \qquad (1)$$

In particular, the proposed correlation is valid for plastic strain levels up to approximately 15%. To validate the obtained results using the correlation in this study, FEM model was constructed using ADINA [5], comprised of the isometric four nodal shell elements assigned to the brace between end plates, Fig. 7 illustrates the used model. The following are dimensional and material properties of the specimen. The yield strength of steel material σ_{yo} was

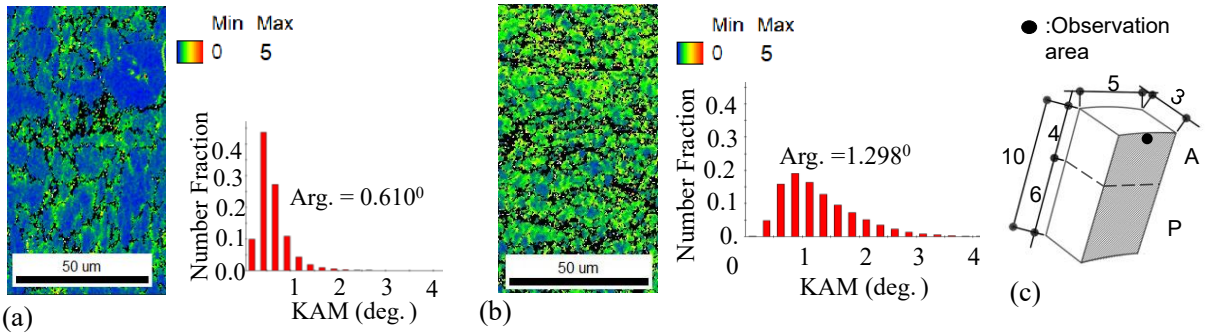

Fig. 6 EBSD Test Results, KAM maps and Frequency: (a) Undeformed Specimen A; (b) Deformed Specimen A; and (c) Specimen A and Sampled Area of Observation.

obtained from the tensile coupon test, while other parameters were calibrated based on cyclic loading tests. Specifically, σ_{yo} and E_p equal to 440 and 110Mpa, respectively were used for isotropic hardening, while h_1 and h_2 of 30000 and 600 Mpa, respectively; and ζ_1 and ζ_2 of 1500 and 8, respectively used for kinematic hardening. Fig. 8 compares the plastic strain values obtained using Eq. (1) with those predicted by FEM results. The measured plastic strain values are considerably high accurate for strain about 15% due to the limitation of the available correlation, the strains with higher values have high variation in comparison to FEM. Eq. (1) and the FEM scheme needs further improvement for plastic strain prediction.

5. Conclusions

Microstructural and mechanical tests on a steel brace subjected to cyclic loading until crack initiation occurred in regions of localized plastic strain. Vickers hardness tests and EBSD analyses were performed to quantitatively evaluate the intensity and distribution of plastic strain in localized areas. The following findings

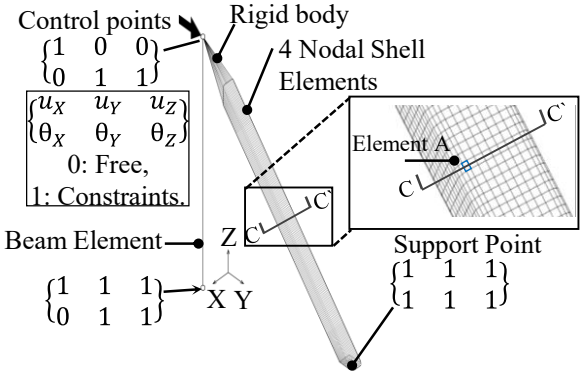

Fig. 7 Steel Brace Model

were obtained:

1. Vickers hardness contour maps revealed a non-uniform hardness distribution across the brace section, with the maximum values concentrated at the brace corners. These regions correspond to areas of plastic deformation and crack initiation.
2. The maximum local plastic strain in the deformed square hollow steel brace was estimated to be approximately 16% to 42%, based on measurements of local grain misorientation obtained from EBSD analysis.

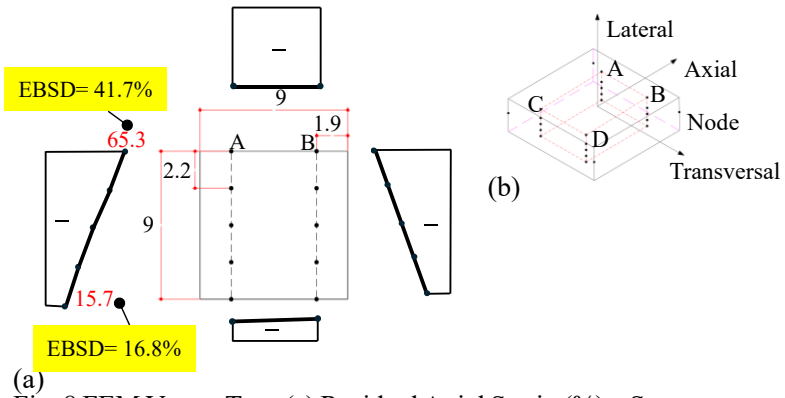

Fig. 8 FEM Versus Test: (a) Residual Axial Strain (%) – Segment AB; and (b) Integration Points in Element A.

Reference

[1] Abe, Y., et al. (2024). Proceedings of Constructional Steel, JSSC, 32, 836–843.

[2] Rui, S.-S., et al. (2018). International Journal of Fatigue, 113, 264–276.

[3] Pavlina, E. J., & Van Tyne, C. J. (2008). Journal of Materials Engineering and Performance, 17(6), 888–893.

[4] Kamaya, M. (2009). Materials Characterization, 60, 125–132.

[5] Bentley systems (2023) Theory and Modeling Guide ADINA 23.00.